Inversion and Application of Seismic Q Factor: Field Dataset Examples.

Wasiu O. Raji, Ph.D.[1*]; Peter I. Olasehinde, Ph.D.[2]; Hussain O. Abubakar, M.Sc.[1]; and Rasheed A. Alabi, B.Sc.[2]

[1]Department of Geology and Mineral Sciences, University of Ilorin, PMB 1515, Ilorin, Nigeria.
[2]Department of Geology, Federal University of Technology, Minna, PMB 65, Niger State, Nigeria.

E-mail: wasiu.raji@gmail.com*

ABSTRACT

In the two previous papers, we introduced a new method for measuring attenuation in reflection seismic data (Raji and Rietbrock, 2013), and a new algorithm for Q-compensation process - to correct the undesirable effects of attenuation in seismograms (Raji and Rietbrock, 2012). We tested the methods with synthetic data examples, and where possible, compared our results with those achieved by other published methods. In this paper, we demonstrate the appropriateness of the Q measuring algorithm and the Q compensation scheme to field dataset, using a set of 3D data recorded in the Gullfaks field, Norway.

The robust features of the Q measuring algorithm include the use of spectral shape factor and variable window length. The shape factor allows the user to represent the real seismic wavelet with several shapes without altering the mathematical formula, while variable window length reduced interference during spectral computation. The average interval $1/Q_m$ calculated from 500 measurements at each of the four time-depth intervals are 0.0196, 0.0573, 0.0389, and 0.0220, for intervals AB, BC, CD, and DE, respectively. Variation in the attenuation structure of the survey area is described with 2D attenuation profiles. Attenuation compensation in field seismograms is also attempted. Q inverse filters are designed for the various earth layers approximated from the seismic traces, using the interval average $1/Q_m$. The inverse Q filtering scheme is applied to the traces one after the other using Matlab programs specifically designed for the study. The compensated data shows higher quality in terms of amplitude size, frequency content and image resolution, compared to the original field data.

(Keywords: seismic Q factor, Q measurement, attenuation compensation, reflection seismic records)

INTRODUCTION

Seismic Q factor is of great interest to exploration geophysicist because it is related to the petrophysical parameters of rocks. Q is related to the porosity and permeability of rocks (Klimentos and McMcan, 1990), saturation level and fluid viscousity. In fact, a study by (Winkler and Nur, 1979) indicates that Q may be more sensitive to the changes in saturation than the velocity. Using Massilon Sandstone, Winkler and Nur show that the effect of saturation on attenuation is greater on the order of magnitude than the effect of saturation on velocity. Q is also sensitive to clay volume, pressure, saturation, and fracture (Winkler and Nur, 1979; Klimentos and McMcan, 1990; Kozlov,2007), and therefore, can be used for lithology discrimination (Parra and hacker, 2006; Dasgupta and Clark, 1998; Singleton, 2008). When cross-plotted with elastic parameters, Q can be used to distinguish oil from gas, and gas from water (Klimentos, 1995; Raji 2012).

Attenuation is a physical phenomenon that describes energy absorption and phase dispersion in elastic waves travelling in rock layers. Attenuation is caused by a wide range of processes that can be grouped into: (i) intrinsic or inelastic attenuation, where a part of the wave energy is converted into heat; and (ii) extrinsic or elastic attenuation, where energy is scattered or redistributed to unobserved wave field. The effects of energy dissipation and phase dispersion often leads to poor seismic data quality, seismic-to-well mistie, and poor migrated images. The degree of attenuation can be approximated from Q measured in seismic data, and the Q can be used to design an attenuation compensation scheme to correct the effects of energy absorption and phase dispersion caused by earth anelasticity. The process of correcting for the effects of seismic attenuation is commonly referred to as Q inverse filtering (Wang, 2002;

2006) or Q-compensation (Raji and Rietbrock, 2012). Q measurement in field seismograms and attenuation correction in recorded seismic data are the key subjects discussed in this paper.

Inversion of seismic Q factor and it application to seismic attenuation compensation is straight forward in synthetic data case. In real data case, the processes are somewhat complex and often lead to undesirable consequences. This is because some of the assumptions in the synthetic seismograms are not always valid in field data cases. The Q measurement algorithm and the attenuation compensation scheme proposed in our previous papers (Raji and Rietbrock, 2012; 2013) discuss, respectively: a new technique for determining seismic attenuation (or seismic Q factor) in reflection seismic data, and a new algorithm for correcting the effects of attenuation in seismic records. (Raji and Rietbrock, 2012; 2013) discussed the theory of attenuation, derived mathematical equations, stated the assumptions, and used synthetic datasets to test the validity of the new Q measurement method and the proposed Q-compensation algorithm. Because the theory of seismic attenuation is more complex than the general theory of wave propagation, the application of these new methods to real dataset is considered necessary in order to show the robustness of the methods, and to prove their acceptability. This paper builds on the knowledge presented in (Raji and Rietbrock, 2012; 2013). It discusses and demonstrates the applications of the mathematical methods previously developed (Raji and Rietbrock, 2012; 2013) to real seismic data acquired in Gullfaks oil field, Norway.

Q is an abbreviation commonly use to designate the seismic quality factor. Seismic Q factor is a measure of the energy dissipation property of rocks. It is commonly used to describe the general property of a rock that contributes to energy reduction in waves. Energy dissipation in a wave due to attenuation can be mathematically defined as:

$$b(x) = b_0 e^{(-\alpha(w)x)}, \quad \textbf{(1)}$$

where b_0 is the initial energy stored in the wave, b is the energy in the wave after travelling a distance x, w is the circular frequency, and α is the attenuation coefficient. The relationship between attenuation coefficient (α) and Q can be defined as:

$$\alpha(w) = \frac{\pi f}{Q(w)v(w)}. \quad \textbf{(2)}$$

Attenuation coefficient (α) is inversely proportional to the seismic quality factor (Q). It can also be stated that the attenuation coefficient is directly proportional to the inverse quality factor ($1/Q$). Due to this relation, $1/Q$ is often used to capture attenuation especially among the rock physicists.

This paper is divided into two parts: The first part describes an application of the method proposed in Raji and Rietbrock (2013) to measuring Q in real seismic data recorded in Gullfaks field; while the second parts discusses the application of the measured Q to correcting the devastating effects of attenuation. Each of the section discusses the results, and the paper ends with conclusion. Details of the mathematical procedure for Q measurement method and Q-compensation algorithm are not discussed in this paper, but are available in the previous papers (Raji and Rietbrock, 2012; 2013).

Inversion of Seismic Q Factor in Reflection Seismic Data

A set of 3D seismic data recorded in Gullfaks Field by STATOIL in 1985 is used for Q measurement. The Gullfaks field is located in the Norwegian sector of the northern North Sea. Figure 1 shows the survey area. The blue rectangle in Figure 1 shows the position of the traces analyzed for Q; the red star shows the position of well A-10; and the blue vertical line represents the traces along CDP 602 line. Traces within the blue rectangle were used for the Q measurement experiment. The traces were edited to remove the traces with unacceptable level of noise. A total of 500 traces were selected for Q measurement.

The section of the data selected for Q measurement is informed by the availability of a well in the area. The well data consist of Time, Porosity, Permeability and Gamma logs covering a depth range of 1500m to 2416m. The information synthesized from the well logs is used to generate lithology and acoustic impedance logs, to provide guidance in discriminating reflections that correspond to lithological boundaries from the signals that are due to artefacts, noise and multiples. Based on this approach, the entire time section covered by the

seismic traces is partitioned into four time-depth intervals: AB, BC, CD, and DE, as shown in Figure 2.

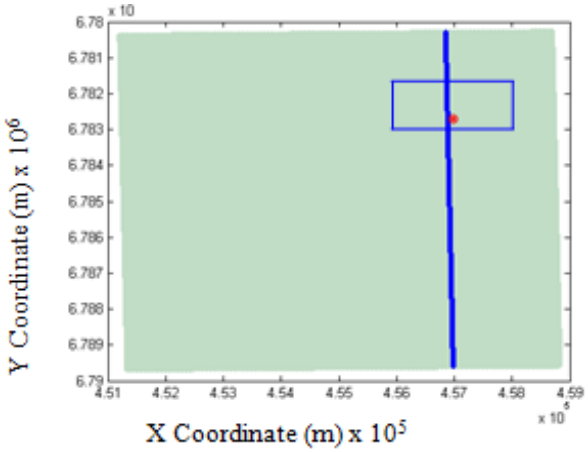

Figure 1: X and Y Coordinates of the survey area. The blue rectangle shows the position of the traces that were analyzed, the red star show the position of the well; and the blue vertical line represents the traces in CDP 602.

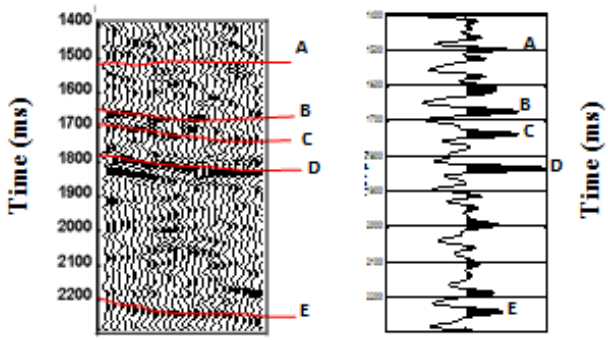

Figure 2: Left- some seismic traces within the blue box in figure 1. Right- stacked trace along the CDP 602 line. The trace length is subdivided into four intervals; AB, BC, CD and DE. The subdivision is for the purpose of Q measurement only.

Q is estimated in the traces using the model proposed by Raji and Rietbrock (2013):

$$Q = \frac{t2cf_a cf_b}{\mu\sigma_{ab}(cf_a - cf_b)}. \qquad (3)$$

Where μ is a constant $(\frac{2\pi}{3})$ representing Ricker wavelet shape factor. t is the vertical time difference between the top and base of the time-depth interval being analyzed; cf_a and cf_b are the centriod frequency of the seismic signal corresponding to the top and base of the interval; and σ_{ab} is the average standard deviation. cf_a and cf_b are defined respectively, as:

$$cf_a = \frac{\int_0^\infty f|a(f)|df}{\int_0^\infty |a(f)|df}; \quad cf_b = \frac{\int_0^\infty f|b(f)|df}{\int_0^\infty |b(f)|df}. \qquad (4)$$

$$\frac{\sqrt{\sigma_a^2} + \sqrt{\sigma_b^2}}{2}. \qquad (5)$$

$$\sigma_{a=}^2 \frac{\int (f-cf_a)^2 a(f)df}{\int a(f)df}; \text{ and } \sigma_{b=}^2 \frac{\int (f-cf_b)^2 b(f)df}{\int b(f)df}. \qquad (6)$$

Seismic signals that correspond to the top and base of the interval to be analyzed for Q were isolated using Hanning windows, and Fourier transform is computed within the window containing each desired seismic signal. To minimize spectral interference, variable window lengths were used (Rein et al., 2009). The minimum and maximum window lengths used are 76ms and 98ms, respectively. Prior to the actual Q measurement, the sensitivity of Q estimate to the window length is tested.

50 traces were used for the window length test. Window size is varied within the minimum and maximum lengths, and Q is measured in the same interval using various window length. Results of the sensitivity test shows that variation in the window length within the maximum and minimum lengths can influence the Q estimates by 2% to 19%. The low error limit is when there is no signal interference (i.e., no noise or multiple within the window). The error increases when there is spectral interference (i.e., when noise or multiples are present within the window).

To reduce signal interference during spectral computation, the minimum possible window length is used in each case. Whenever possible, the same window length is used for a signal pair being compared for Q measurement. Important step before computing the spectral parameters is the accurate time measurement of the reflection events. The definition of arrival time adopted is the travel time that corresponds to the maximum amplitude of the desired seismic event. The time t used for the Q inversion is the difference between travel time of a paired events – one event corresponding to the top, and the other

corresponding to the bottom of the interval being analysed for Q. Examples of the frequency spectral of seismic signals computed at the top and bottom of interval BC in one of the traces are shown in Figure 3.

A total of 2000 Q values were measured- 500 measurements at each of the four time-depth interval. The distributions of Q measured at each interval are shown in Figure 4. The mean inverse Q ($1/Q_m$) is calculated as:

$$\frac{1}{Q_m} = \frac{1}{n}\sum_{i=1}^{n}\frac{1}{Q_i}. \quad \textbf{(7)}$$

Where $\frac{1}{Q_i}$ is the inverse of the individual Q value. i = 1, 2, 3, 4, 5, ..., n, where n is 500.

The negative values of Q were considered as outliers and therefore were excluded from the computation of $1/Q_m$.

The outliers constitute less than 5% of the total estimates (see Figure 4). The profile of $1/Q_m$ and the standard deviation, σ calculated for each interval are plotted in Figure 5.

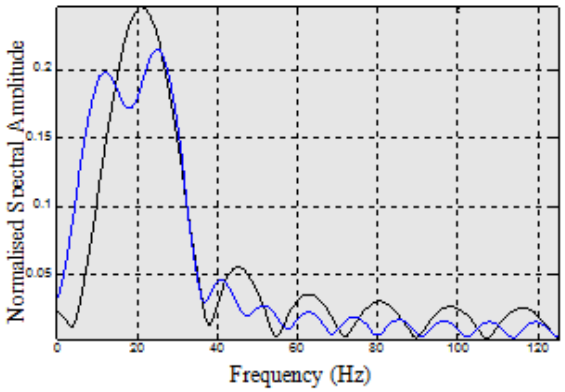

Figure 3: The frequency spectrum of the seismic signals corresponding to the top (black) and bottom (blue) of interval BC in one of the traces.

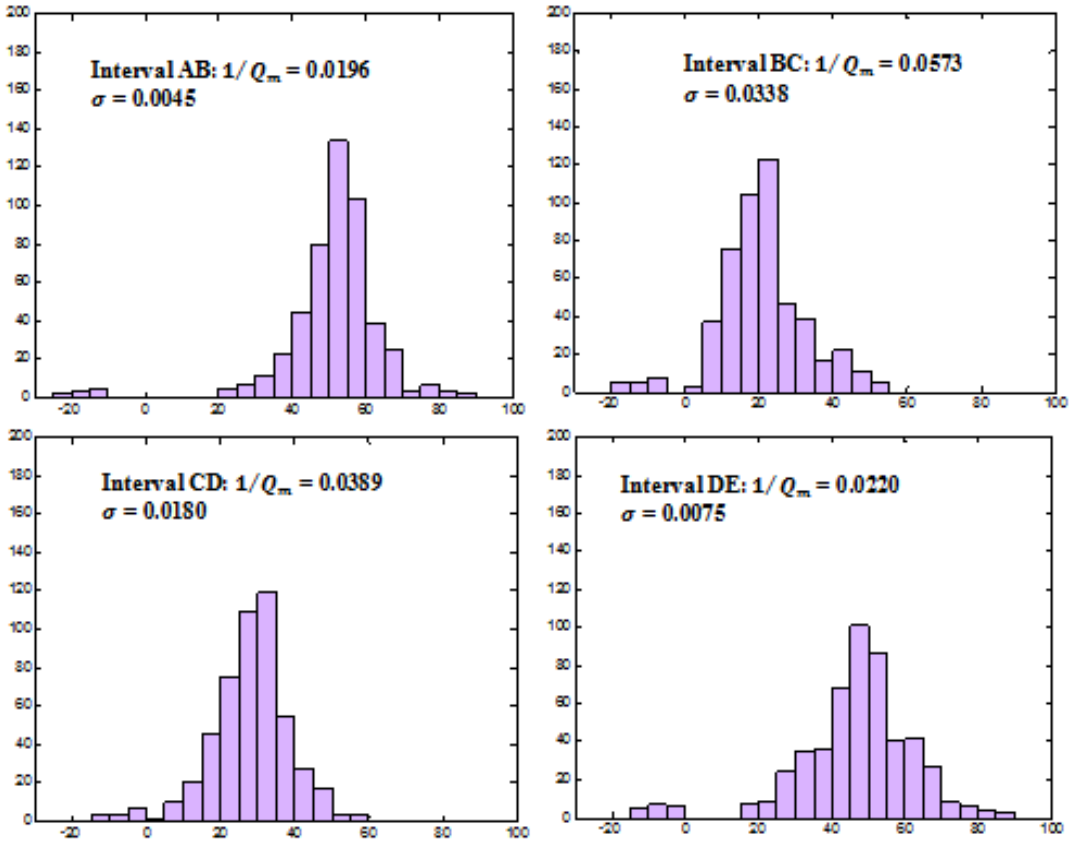

Figure 4: Histograms showing the distribution of the Q estimates at the four intervals. The negative values of Q are not considered in the computation of the mean attenuation ($1/Q_m$).

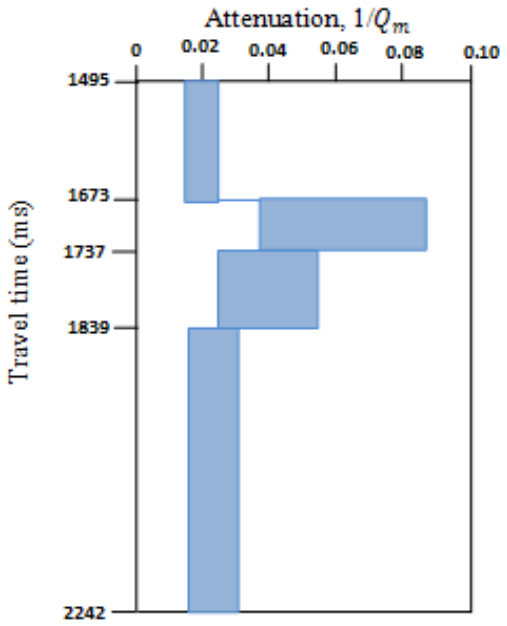

Figure 5: Attenuation profile plotted from the $1/\mathbf{Q_m} \pm \sigma$ calculated from the positive values of Q shown in Figure 4.

To confirm the reliability of the method used in this paper, the method (here known as Q inversion method, QIM) is compared with a well referenced Q estimation method, the Spectral ratio method, SRM.

The traces corresponding to CDP 602 (blue line in Figure 1) are stacked and attenuation (or 1/Q) is measured in the stacked traces using the QIM and SRM. The attenuation profile plotted from 1/Q measured in the stack traces using QIM and SRM are shown in Figure 6.

Discussion of Results 1: Inversion of Seismic Q factor in Reflection Seismic Data

Q measurements were performed on 500 traces selected from the seismic data recorded in the Gullfaks field, North Sea, Norway using the method proposed by Raji and Rietbrock (2013). The data length is partitioned into four time-depth sections: AB, BC, CD, and DE. The estimated mean attenuation ($1/Q_m$) are 0.0196, 0.0573, 0.0389, and 0.0220, while the standard deviation (σ) of the mean estimates are 0.0045, 0.0338, 0.0180, and 0.0075, respectively. The attenuation profile plotted from the 1/Q measured in the CDP-stacked trace (Figure 6), using QIM and SRM are comparable, and they agree qualitatively with the attenuation profile plotted from the $1/Q_m$ (Figure 5).

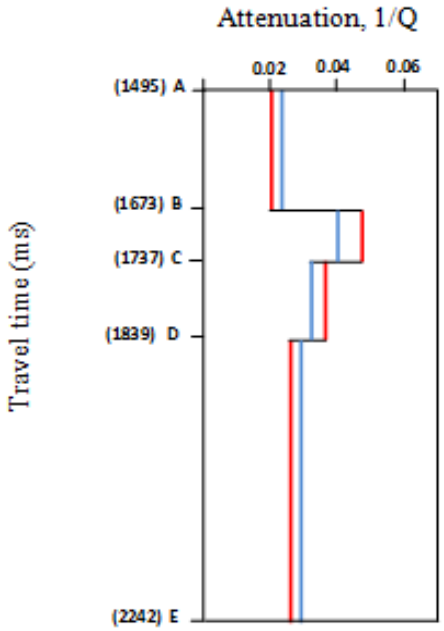

Figure 6: Attenuation profile plotted from the 1/Q estimated from the stacked trace. Red is from QIM, blue is from SRM.

The mean attenuation $1/Q_m$ computed from the 500 measurements and $1/Q$ measured in the traces stacked along the CDP 602 line show that interval BC has the highest attenuation value, and that interval AB has the lowest attenuation value. The values of $1/Q_m$ and $1/Q$ measured in interval BC by QIM are 0.0573 and 0.0489, respectively. While the $1/Q_m$ and 1/Q measured at interval AB are 0.0196 and 0.0202, respectively. Interval BC which recorded the highest attenuation value approximately coincides with the shale break that separates the top and base sandstones. The factor responsible for high attenuation in interval BC compared to the overlying and underlying sandstone cannot be ascertained from this study.

However, results from attenuation measurement by Stainsby and Worthington (2009) in VSP data recorded in a well from North Sea, Norway, show that shale in the area has a Q value of 25 ± 3 (i.e., $0.0357 \leq 1/Q \leq 0.0455$). Toverud and Ursin, 2005 also show that Q values in sandstone of the North Sea Norway ranges between 30 and 40 (i.e., $0.0250 \leq 1/Q \leq 0.0333$). These figures are

in considerable agreement with those recorded by this study.

Application of Seismic Q Factor to Seismic Image Improvement

When Q is successfully determined in seismic data, it can be incorporated into an inverse filter to correct energy absorption and phase dispersion caused by attenuation. The process of correcting for energy absorption and phase dispersion is known as attenuation compensation or Q-compensation. Q-compensation can be achieved by a means of Q-inverse filtering, a process that can be described as reversed attenuation. The issue confronting Q inverse filtering algorithms is instability (Wang, 2002; Li et al., 2009).

Instability is a common problem –a natural consequence of inverse Q filtering process. It is usually due to overflow or numerical instability in the estimation of the exponential functions, especially at high travel time components of the inverse Q-filtered traces. This problem often leads to the introduction of artifacts and the amplification of ambient noise in the Q inverse filtered traces.

When tested with synthetic seismic traces, the algorithm (Raji and Rietbrock, 2013) circumvents the issue of numerical instability and prevents the introduction of artifacts that usually mar the results of an inverse Q-filtering process. In this section of the paper, we test the appropriateness of the algorithm to real seismogram, using a 3D data set recorded in the Gullfaks field, Norway.

To make a complete sense to readers who have not read our previous paper (Raji and Rietbrock, 2012) that discussed the detailed theory of Q-compensation, or other paper on similar topic (Wang, 2002; 2006; Bickel and Natarajan, 1985; Hargreaves and Calvert, 1991; Mittet et al., 1995). We summarize the process of seismic attenuation (the problem) and attenuation compensation (the solution) using the basic equations, and show the improvements in synthetic seismic traces due to attenuation compensation, before moving on to apply the Q-compensation algorithm to field seismic data.

The process of seismic energy absorption in a wave, A_0 at position z after travelling a distance Δx in an attenuating medium of seismic quality factor, Q can be described as:

$$A_1(z+\Delta z,w) = A_0(z,w)\exp(-j\frac{w}{\beta(w)}\Delta z)\exp(-\frac{w}{2\beta(w)Q}\Delta z) \quad \textbf{(8)}$$

Where j is the imaginary number, w and w_c are the angular frequency and the reference angular frequency, respectively. – Sign shows that the wave is travelling in the forward direction (from the source to the reflector).

$\beta(w)$ is the frequency dependent velocity. The two exponential operators in (3) describe phase dispersion and amplitude reduction, respectively. $\beta(w)$ is related to the real valued layer velocity (v) as:

$$\beta(w) = v(1-(\pi Q)^{-1}\ln\left(\frac{w}{w_c}\right)). \quad \textbf{(9)}$$

Where π is a constant. To compensate for seismic energy absorption (amplitude diminution) and phase dispersion, arising from attenuation of wave A_1, an inverse Q -filter must be applied to A_1. A basic inverse Q filtering or Q compensation scheme is defined as:

$$(z+\Delta z,w) = A_0(z,w)\exp(j\frac{w}{\beta(w)}\Delta z)\exp(\frac{w}{2\beta(w)Q}\Delta z) \quad \textbf{(10)}$$

The two exponential operators in equation 10 correct the effects of velocity dispersion and amplitude diminution, respectively. The Q compensation scheme is tested on synthetic seismic traces computed from an eight-layer earth model. Time domain traces are transformed to Fourier domain, and the Q-compensation scheme is applied in the Fourier domain.

Figure 7a shows attenuated seismic traces while Figure 7b shows the traces after the application of Q compensation scheme described in Equation 10.

The basic concept of the Q-compensation scheme is to correct for the effects of attenuation from the source point to the receiver location. The procedure is analogous to reversing the direction of propagation: starting from the receiver, backward-propagate the wave to the reflector and then, to the source.

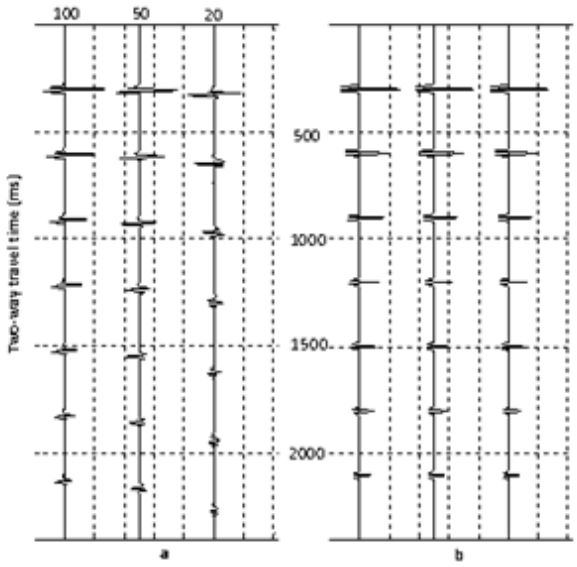

Figure 7: Synthetic seismic traces before and after Q-compensation: **(a)** constant Q attenuated traces. Q values are 100, 50 and 20 for the first, second and third trace, respectively. **(b)** The respective trace after Q-compensation.

By this procedure the wave is corrected for the attenuation it encountered in the down-going direction (from source to reflector) and up-going directions (from reflector to receiver). During inverse Q compensation process, each layer is treated as a single homogenous entity; the attenuated signal corresponding to the layer boundary is isolated in the time domain using wavefield extrapolation; the signal is treated with the inverse Q-filter in the frequency domain; and stored in the time domain. The output of the compensation scheme is a trace formed by the summation of compensated signals representing all layers in the earth model. The inverse Q-filter at a layer step 3, for an example, contains the Q factor that is responsible for the attenuation experienced by the wave in the previous and current layers.

$$A_3(T_3, w) = A_2(T_2, w) \exp\left(j\frac{w\Delta T_3}{\beta_3(w)}\right) \exp\left(\frac{w\Delta T_3}{2\beta_3(w)Q_3}\right)$$

where T is the trave ltime, and $\Delta T_3 = T_3 - T_2$.

Further, the Q compensation scheme is applied to 3D seismic reflection data. A trace from the 3D data set before and after Q-compensation is shown in Figure 8. The entire trace used for the Q-compensation test is shown in Figure 9. The top plot shows the original traces before Q-compensation, while the bottom plot is the traces after Q-compensation. The reflectors in the compensated trace are sharper and better resolved than the reflectors in the original traces. To show that inverse Q filtering process boosts the frequency component of the wave, a comparison of the average frequency spectrum of seismic traces before and after Q-compensation is shown in Figure 10. The blue spectrum which represents the frequency of the Q-compensated traces shows higher peak frequency than the black spectrum which represents the original traces. The blue spectrum also shows the restoration of high frequencies (70Hz-120Hz) that have been absorbed in the black spectrum. The traces are plotted in pixel format in Figure 11, and the difference between the compensated and original (attenuated) traces is also plotted in pixel format in Figure 12. The Q-compensation process corrected amplitude diminution caused by energy absorption by restoring the absorbed amplitude; it also enhanced the frequency content of the traces, and thereby corrects phase dispersion; and consequently gives a clearer image of reflectors. Overall, the Q-compensation process improves the interpretability of the data.

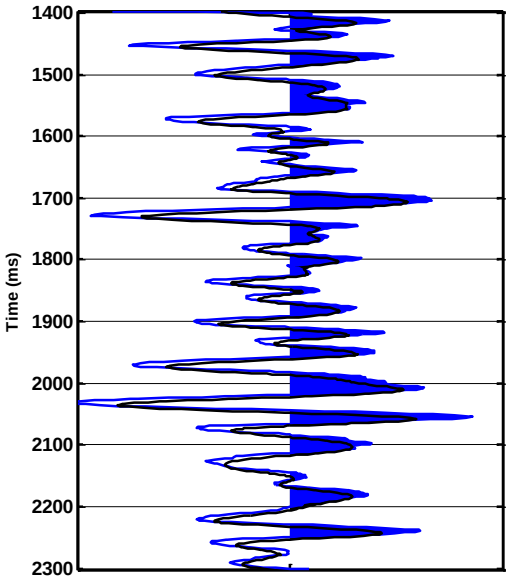

Figure 8: Attenuated and compensated seismic traces-showing the effects of seismic Q compensation. Black is original (attenuated) traces, blue is after Q compensation.

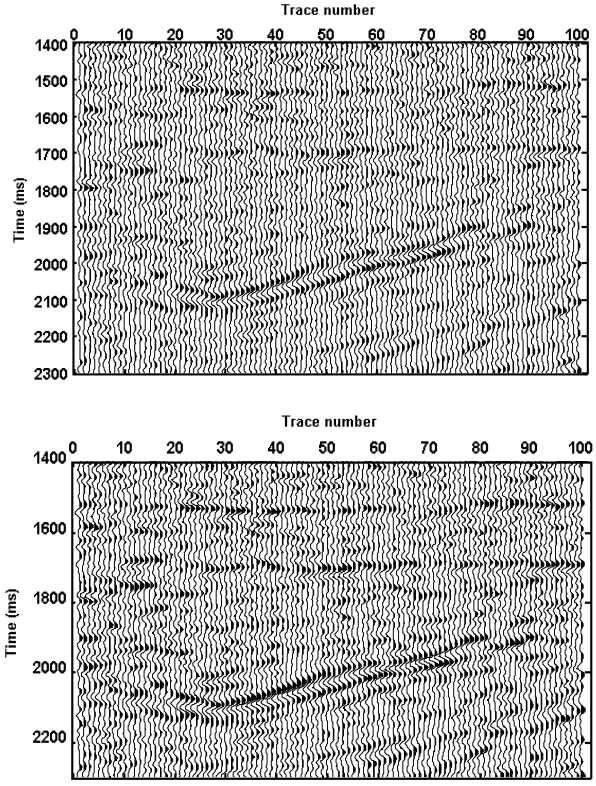

Figure 9: Field traces plotted in wiggle format- showing clearer image of the reflectors after Q-compensation. (Top) original field traces, (bottom) Q-compensated traces.

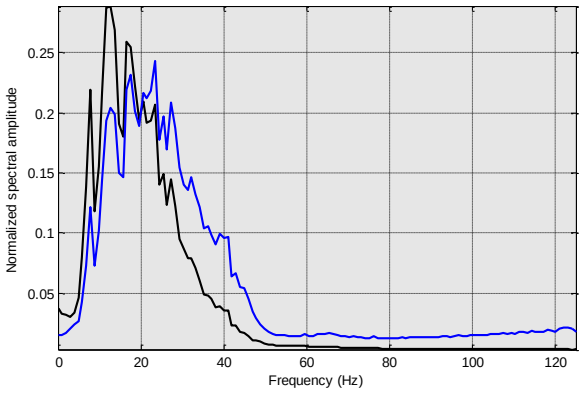

Figure 10: The mean spectrum of the traces - showing restoration of high frequencies in the compensated traces (blue) compared to the uncompensated traces (black). The High frequency components that have been attenuated in the original trace have been restored in the compensated traces.

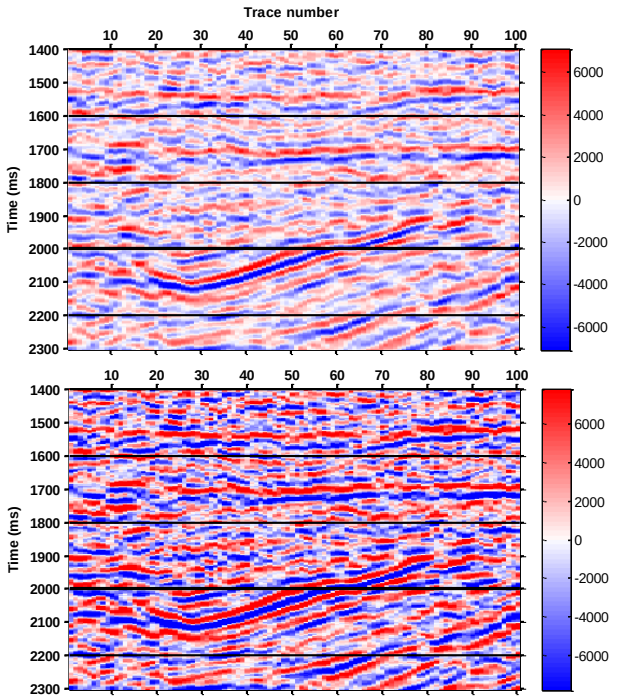

Figure 11: Time-amplitude data plotted in pixel format. (Top) the original traces before Q-compensation, (bottom) traces after Q-compensation.

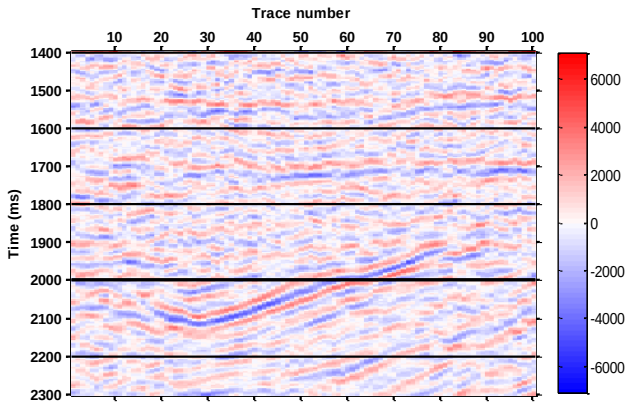

Figure 12: The difference plot between the compensated and original data- showing the improvement in the seismic image achieved by the Q compensation process.

Discussion of Results 2: Application of Seismic Q Factor to Seismic Image Improvement

Q inverse filtering is a seismic enhancement process that consists of three key processes: estimation of the seismic Q-factor; design of stable Q-inverse filter; and application of the Q-inverse filter to seismic traces. The proposed algorithm proved appropriate when applied to synthetic seismic data computed from various Earth Q models, and field data acquired in the Gullfaks Field. It circumvents the issue of instability and prevents the introduction of artefacts – the general problem of inverse Q filtering. For Q compensation in field data, 500 estimates of Q were done at four time-depth intervals, and the average interval attenuation ($1/Q_m$) is used to designed the respective inverse filter. Following this, the Q inverse filter is applied to the traces one after the other.

At first, synthetic traces from eight layered earth model are used to show the improvement achievable in seismic data by the application of the proposed Q-compensation algorithm (Raji and Rietbrock, 2012): the Q-compensated synthetic traces show higher amplitude compared to the original traces. When applied to reflection dataset from Gullfaks Field, North Sea Norway, the data shows restoration of high frequency energy that have been absorbed in the original data due to attenuation. It also shows clearer images of the reflectors at the accurate time-depth. The overall consequence of the processed is high quality data.

CONCLUSION

The use of synthetic data set for seismic Q factor measurement and Q-compensation is somewhat easy and straightforward in synthetic data case. In real data case, Q measurement and Q-compensation are usually complex, because the assumptions in the synthetic case are not always valid in real data cases. Using field data example, we show the robustness of the Q measurement method in pre-stack and stacked field seismic data. Consistencies in the interval 1/Q measured in the pre-stack and stacked data confirm the appropriateness of our method. The reliability of our results is corroborated by attenuation data previously published for the study area. The average interval $1/Q_m$ calculated from our results is used to implement Q-compensation procedure by a means of inverse filtering scheme applied to the field seismic traces one after the other. The Q- inverse filtering scheme overcame the problem of instability without introducing artifacts, corrected the effect of energy absorption and phase dispersion caused by attenuation. Consequent, the Q inverse filtered traces gave clearer images of subsurface structures with enhanced frequency content and signal amplitudes.

REFERENCES

1. Bickel, S.H. and R.R. Natarajan.1985. “Plane Wave Q Deconvolution”. *Geophysics*. 50:1426 – 1439.

2. Dasgupta, E.A. and R.A. Clark.1998. “Estimation of Q from Surface Seismic Data”. *Geophysics*. 63: 2120- 2128.

3. Hargreaves, N.D. and A.J. Calvert. 1991. “Inverse Q Filtering by Fourier Transform”. *Geophysics*. 56: 519-52.

4. Klimentos, T. 1995. “Attenuation of P-Wave and S- Wave as a Method of Distinguishing Gas Condensate from Oil and Water”. *Geophysics*. 60: 447 -458.

5. Klimentos, T. and C. McCann. 1990. “Relationships between Compressional Wave Attenuation, Porosity, Clay Content and Permeability of Sandstones”. *Geophysics*. 55: 998–1014.

6. Knight, R., J. Dvorkin, and A. Nur. 1998. “Acoustic Signature of Partial Saturation”. *Geophysics*. 63:132-138.

7. Kozlov, E. 2007. “Seismic Signature of a Permeable, Dual Porosity Layer”. *Geophysics*. 72: SM281- SM291.

8. Li, H.Q., B. Zhao, B.W. Tang, W.C. Wang, and H.Y. Zhang. 2009. “Q-Absorption Compensation-an Application Study”. Expanded Abstract, 70th Annual International Meeting of the European Association Geoscientists and Engineers.

9. Mittet, R., R. Sollie, and K. Hokstad. 1995. “Prestack Depth Migration with Compensation for Absorption and Dispersion”. *Geophysics*. 50:1485-1494.

10. Parra, O.J., C.L. Hackert, L. Wilson, H.A. Collier, and T. Thomas. 2006. “Q as a Lithologic and Hydrocarbon Indicator: from Full Waveform Sonic

to 3D Surface Seismic". Report no: DE-FC26-02NT15343.

11. Raji, W.O. 2012. "Rock Physics Diagnostics, Attenuation Measurement and Analyses in Wells". *Geosciences*. 2(6): 170-178.

12. Raji, W.O. and A. Rietbeock. 2012. "Enhanced Seismic Q Compensation I: Algorithm Formulation and Synthetic Application". *Frontiers in Science*. 2(6):243 – 249.

13. Raji, W.O. and A. Rietbrock.. 2013. "Attenuation (1/Q) Estimation in Reflection Seismic Records". *Journal of Geophysics and Engineering*. 10(4): 045012.

14. Reine, C., M. Van Dan Baan, and R. Clark. 2009. "The Robustness of Seismic Attenuation Measurement using Fixed and Variable-Window Time-Frequency Transform". *Geophysics.* 74: WA123-WA135.

15. Singleton, S. 2008. "The use of Seismic Attenuation to Aid Simultaneous Impedance Inversion in Geophysical Reservoir Characterisation". *The Leading Edge*. 27:398–407.

16. Stainsby, S.D. and W.H.Q. Worthington. 1985. "Attenuation Estimation from Vertical Seismic: Profile Data and Anomalous Variation in the Central North Sea". *Geophysics*. 50:615–626.

17. Toverud, T. and B. Ursin. 2005. "Comparison of Seismic Attenuation Models using Zero-Offset Vertical Seismic Profiling (VSP) Data". *Geophysics*. 70: F17-F25.

18. Wang, Y. 2002. "A Stable and Efficient Approach of Inverse Q Filtering". Geophysics. 67:657–663.

19. Wang, Y. 2006. "Inverse Q Filter for Seismic Resolution Enhancement". *Geophysics*. 71: V51-V60.

20. Winkler, K. and A. Nur. 1979."Pore Fluids and Seis Micattenuation in Rocks". *Geophysical Research Letter*. 6: 1 – 4.

ABOUT THE AUTHORS

Wasiu O. Raji, is a Lecturer at the University of Ilorin, Nigeria. He holds a Ph.D. in Earth Science from the University of Liverpool, U.K. He's currently a Postdoctoral Researcher at Stanford University, Geophysics Department, California, U.S. His research interest includes seismic inversion, seismic signal processing, and rock physics.

Peter Olasehinde, is a Professor of Geophysics at the Federal University of Technology, Minna, Nigeria. His research interest includes ground water exploration and hydro-geochemistry.

Hussain Abubakar, holds a B.Sc. in Geology, M.Sc. in GIS and PGD in Geophysics. He's currently enrolled in a Master's program in Geophysics.

Alabi Rasheed, holds a B.Sc. in Geology and he currently enrolled in a Master's program in Geophysics. He has industry experience in the area of ground water exploration.

SUGGESTED CITATION

Raji, W.O. P.I. Olasehinde, H.O. Abubakar, and R.A. Alabi. 2014. "Inversion and Application of Seismic Q Factor: Field Dataset Examples". *Pacific Journal of Science and Technology*. 15(1):318-327.

Pacific Journal of Science and Technology